

1 **Earth's new tectonic regime at the dawn of the**
2 **Paleoproterozoic: Hf isotope evidence for efficient**
3 **crustal growth and reworking in the São Francisco**
4 **Craton, Brazil**

5 **Henrique Bruno^{1,2}, Monica Heilbron¹, Rob Strachan², Mike Fowler², Claudio de**
6 **Morisson Valeriano¹, Samuel Bersan^{1,2}, Hugo Moreira², Kathryn Cutts¹, Joseph**
7 **Dunlop², Rasec Almeida¹, Julio Almeida¹, Craig Storey²**

8 ¹ – *Tektos- Grupo de Pesquisa em Geotectônica, Universidade do Estado do Rio de*
9 *Janeiro, Faculdade de Geologia. Rua São Francisco Xavier 524, Maracanã, Rio de*
10 *Janeiro, Brazil.*

11 ² – *University of Portsmouth, School of the Environment, Geography and Geosciences,*
12 *Burnaby Building, Burnaby Road, Portsmouth, PO1 3QL, UK.*

13 **ABSTRACT**

14 A zircon Hf isotopes dataset of Archean and Paleoproterozoic magmatic and
15 metasedimentary rocks of southern São Francisco Craton is interpreted as evidence of
16 accretionary and collisional plate tectonics at least since the Archean-Proterozoic
17 boundary. During the Phanerozoic, accretionary and collisional orogenies are considered
18 the end members of different plate tectonic settings, both involving pre-existing stable
19 continental lithosphere and consumption of oceanic crust. However, mechanisms for the
20 formation of continental crust during the Archean and Paleoproterozoic are still debated
21 with the addition of magmatic rocks to the crust being explained by different geodynamic
22 models. Hf isotopes can be used to quantify the proportion of magmatic addition into the
23 crust: positive ϵ_{Hf} values are usually interpreted as indications of magmatic input from
24 the mantle, whereas crust-derived rocks show more negative ϵ_{Hf} . We show that the crust
25 of the amalgamated Paleoproterozoic tectonostratigraphic terranes that make up the
26 southern São Francisco craton were generated from different proportions of mantle and
27 crustal isotopic reservoirs. Plate tectonic processes are implied by a consistent sequence
28 of events involving the generation of juvenile subduction-related magmatic arc rocks,

29 followed by collisional orogenesis and re-melting of older crust, and post-collisional
30 bimodal magmatism.

31 INTRODUCTION

32 Whether plate tectonic processes initiated around the Archean-Paleoproterozoic
33 boundary or at a different point in Earth's evolution is intensely debated (e.g., Dhuime et
34 al., 2012; Windley et al., 2020; Palin and Santosh, 2020). Hf isotopes provide an
35 important tool for understanding tectonic processes through time because magmatic
36 sources can be identified by the contrasting isotopic behaviour of Hf between the mantle
37 and the crust (Griffin et al. 2000). Secular changes in orogenic processes can be traced by
38 Hf isotope variations, as the isotopic signature of magmatic zircon crystals is usually
39 related to their petrogenesis, thereby indicating degrees of mantle contributions and
40 crustal sources and thus constraining the predominant magmatic and tectonic style (e.g.,
41 Goodge and Vervoort, 2006; Belousova et al., 2010; Dhuime et al., 2012; Spencer et al.,
42 2019, 2020).

43 Different $\epsilon\text{Hf}/\text{Ma}$ trajectories and $^{176}\text{Lu}/^{177}\text{Hf}$ ratios are key in determining
44 changes in tectonic environment (Kemp et al., 2007; Laurent and Zeh, 2015; Spencer et
45 al., 2019). Two end members of orogenic cycles can be distinguished by their contrasting
46 Hf evolution patterns: 1) collisional orogens arising from the collision of two or more
47 continental blocks and resulting in reworking of crustal material, and 2) accretionary
48 orogens containing a high component of juvenile material related to the amalgamation of
49 island arcs (eg. Belousova et al., 2010; Collins et al., 2011; Spencer et al., 2019, 2020).

50 We use Hf isotopes in zircon grains to determine the proportion of juvenile and
51 reworked material in the studied samples and to interpret the tectonic framework of a
52 Paleoproterozoic orogenic system in southeastern Brazil (the Minas Segment of the

53 Minas-Bahia Orogenic System). The variations in the dataset show an intense reworking
54 of older continental fragments as well as major input of mantle-derived magmas
55 comparable with the isotopic evolutionary trend of Neoproterozoic and Phanerozoic
56 orogenic systems. The resemblance with modern-style plate tectonic processes indicate
57 that similar mixing mechanisms have operated throughout the last 2.4 billion years of
58 Earth's history.

59 **TECTONIC FRAMEWORK OF A PALEOPROTEROZOIC OROGENIC** 60 **SYSTEM**

61 The Precambrian basement of Brazil comprises Archean-Paleoproterozoic cratons
62 that were amalgamated during the ca. 0.6-0.5 Ga Brasiliano-Pan African orogeny and
63 later covered by Phanerozoic intracontinental basins (Figure 1a) (e.g., Heilbron et al.,
64 2017). The São Francisco Craton (SFC) mainly composed of Archean blocks and
65 Paleoproterozoic arc-related rocks, and its reworked inliers within the Neoproterozoic
66 belts, formed during one of the most important periods of juvenile crust addition and
67 reworking, expressed by Siderian to Rhyacian accretional to collisional episodes. On the
68 eastern side of the SFC, the Paleoproterozoic orogenic belt known as the Minas-Bahia
69 Orogenic System (MBOS) is subdivided into two segments: the northern (Bahia)
70 segment, which outcrops in the interior of the cratonic area, and the southern (Minas)
71 segment, exposed on the southern tip of the SFC as well as in reworked basement inliers
72 occurring in the Neoproterozoic orogenic systems (e.g., Alkmim and Teixeira, 2017;
73 Teixeira et al., 2017) (Figure 1b).

74 The Minas segment of the MBOS (ca. 2.47-2.05 Ga) represents a myriad of
75 microcontinents and magmatic arcs, including mainly intra-oceanic, largely juvenile
76 accretionary arcs that were diachronously amalgamated between ca. 2.1 and 2.05 Ga (e.g.,
77 Heilbron et al., 2010; Ávila et al., 2014; Alkmim and Teixeira, 2017; Araújo, 2020; Bruno

78 et al., 2020, 2021; Cutts, et al., 2020). From west to east they are regarded as (Figure 1c):
79 1) Archean complexes encompassing Paleo- to Neoproterozoic tonalite-trondhjemite-
80 granodiorite (TTG), migmatites, high-K meta-granitoids, greenstone belt sequences (e.g.,
81 Rio das Velhas Supergroup) of ca. 2.9 to 2.65 Ma and Archean-Paleoproterozoic
82 supracrustal units of the passive to active margin type of the Minas Supergroup; 2) the
83 Mineiro magmatic arc comprising Siderian to Rhyacian juvenile to crust-contaminated
84 magmatic arc granitoid rocks including high Ba-Sr, TTGs, sanukitoids and hybrid
85 granitoids and related supracrustal units; 3) the Archean Piedade microcontinent, with
86 Neoproterozoic TTG and sanukitoids intruded by ca. 2.5 Ga intraplate alkaline basic rocks;
87 4) ca. 2.05 Ga post-collisional granitoids and associated tholeiitic metabasics; and 5) the
88 Mantiqueira, ca. 2.2 Ga to ca. 2.0 Ga, and Juiz de Fora magmatic arcs, ca. 2.4 to 2.07 Ga,
89 which are represented by juvenile to crustal contaminated TTGs, sanukitoids, post-
90 collisional alkaline, within-plate tholeiitic basic rocks and peraluminous granitoid rocks
91 (e.g. Heilbron et al., 2010; Ávila et al., 2014; Alkmim and Teixeira, 2017; Teixeira et al.,
92 2017; Degler et al., 2018; Moreira et al., 2018; Bruno et al., 2020, b; Cutts et al., 2020;
93 Araújo, 2020).

94 **LU-HF SIGNATURES OF THE MINAS SEGMENT OF THE MBO**

95 Analytical methods, sample descriptions/locations, U-Pb and new Lu-Hf isotope
96 data are presented in Supplementary Materials A and B. Fifteen samples that represent
97 the chemical diversity of the Paleoproterozoic magmatic arcs and Archean
98 microcontinent were chosen for Hf isotopic analysis (Figure 2). The Lu-Hf analyses were
99 performed on concordant to sub-concordant zircon grains directly on U-Pb spots (when
100 possible). Analyses were performed using an ASI Resolution SE 193 excimer laser
101 connected to a Nu Plasma I MC-ICP-MS. For old and complex terranes, such as the São

102 Francisco Craton, model ages values (TDM) have been used in a rather qualitative way
103 to support geological interpretation (eg. Vervoort and Kemp, 2016; Spencer et al., 2020).

104 Lu-Hf analyses of Neoproterozoic rocks of the Piedade microcontinent (Samples 50,
105 66A and 66B) show a range of ϵHf (crystallization age) from approximately chondritic (-
106 0.65) to crustal (-8.70) values, suggesting an even older Archean substratum into which
107 these rocks were intruded or derivation from a source of that age within the crust (Figure
108 2). Paleoproterozoic metamorphic rims were also analyzed and yield ϵHf (at metamorphic
109 age) of -12.23 and -22.10 further suggesting crustal reworking (Figure 2). The $^{176}\text{Hf}/^{177}\text{Hf}$
110 ratios versus the crystallization age of the zircon grains display values ranging ranging
111 from 0.28089 ± 0.00003 to 0.28114 ± 0.00003 for the magmatic cores and for the
112 metamorphic rims, which are coincident within uncertainty and thus likely represent
113 simple recrystallisation under metamorphic conditions or new zircon with more negative
114 ϵHf reflecting the increase of $^{176}\text{Hf}/^{177}\text{Hf}$ in CHUR (Figure 2). TDM values vary from
115 Paleo- to Mesoproterozoic ages ca. 3.55 to 3.01 Ga.

116 The Rhyacian (ca. 2.152 to 2.114 Ga) arc-related granitoids of the Mineiro
117 magmatic arc (Samples 42, 51B and 52B) show $^{176}\text{Hf}/^{177}\text{Hf}$ values of 0.28128 ± 0.00002
118 and 0.28159 ± 0.00002 with juvenile and crustal ϵHf (crystallization age) values of +5.84
119 and -5.52 and TDM of ca. 2.81 and 2.16 Ga, that together with the presence of Archean
120 zircon inheritance in Sample 51B, indicate a mixed mantle-crust evolution of this
121 Paleoproterozoic magmatic arc.

122 Sample 67, from the Mantiqueira magmatic arc, yields chondritic to juvenile ϵHf
123 (crystallization age) of +1.68 to +0.57 whereas samples 8 and 64 B yield more evolved,
124 and therefore crust-contaminated values of ϵHf (crystallization age) between -3.40 and -
125 8.68 (Figure 2). The $^{176}\text{Hf}/^{177}\text{Hf}$ values of the samples vary between 0.28117 ± 0.00003

126 and 0.28149 ± 0.00003 , with TDM varying from 3.25 to 2.32 Ga, also indicating a
127 complex evolutionary history (Figure 2).

128 The Paleoproterozoic samples of the Piedade microcontinent (Samples 58A, 58B,
129 65, 68A and 70B), related to the post-collisional setting of the Minas segment of the
130 MBOS yield negative values of ϵ_{Hf} values (at crystallization age) between -7.21 and -
131 20.92, implying reworking of older continental crust. Inherited zircon grains were also
132 analyzed showing an evolutionary trend of the isotopic reservoir of the Piedade
133 microcontinent from the Archean towards the Paleoproterozoic (Figure 2). The model
134 ages show Archean signatures varying from ca. 3.52 to 2.82 Ga and $^{176}\text{Hf}/^{177}\text{Hf}$ ratios
135 from 0.28083 ± 0.00003 to 0.28128 ± 0.00002 . Sample 70A, a tholeiitic metabasic rock,
136 of ca. 2.05 Ga displays variable ϵ_{Hf} (crystallization age) of -17.63 to +2.63 implying a
137 juvenile addition with crustal reworking related to an extensional setting, indicating the
138 mixed crustal-mantle sources for the post-collisional bimodal magmatism (Figure 2).

139 **A PROTRACTED MIXED ACCRETIONARY TO COLLISIONAL OROGENIC** 140 **CYCLE**

141 Linear ϵ_{Hf} -time arrays can be indicative of long-term evolution trends from a
142 singular isotopic source (e.g., Rudnick and Gao, 2003; Laurent and Zeh, 2015; Spencer
143 et al., 2019). With reference to the time intervals of ca. 2.5 - 2.4 Ga, 2.4 -2.3 Ga, 2.2 - 2.1
144 Ga and 2.1-2.0 Ga, the values of $\epsilon_{\text{Hf}}/\text{Ma}$ trajectories and $^{176}\text{Lu}/^{177}\text{Hf}$ are regarded as
145 reflecting the main periods of juvenile input and reworking, marked by collisional
146 episodes, as shown by the probability regressive line of juvenile and crust-contaminated
147 samples (Figure 3a).

148 The interval of ca. 2.5 – 2.4 Ga, represents the initial stages of magmatic arc
149 granitoid rocks generation in the MBOS with mainly crust-contaminated isotopic

150 signatures ($\epsilon\text{Hf}/\text{Ma} = 0.00793$). The ca. 2.4 – 2.3 Ga interval ($\epsilon\text{Hf}/\text{Ma} = -0.05784$),
151 reflects the onset of juvenile magmatism in the Mineiro and in the Juiz de Fora magmatic
152 arcs. The interval of ca. 2.2 - 2.1 Ga ($\epsilon\text{Hf}/\text{Ma} = 0.00752$) reflects the main period
153 magmatic arc granitoid rocks generation in the MBOS whereas ca. 2.1-2.0 Ga ($\epsilon\text{Hf}/\text{Ma} =$
154 0.13384) reflects the collisional episodes of MBOS with mostly crustal recycling (Figure
155 3 a). For the whole Paleoproterozoic continental crust evolution of the MBOS, analyses
156 of igneous magmatic zircon grains of the Mineiro, Mantiqueira and Juiz de Fora
157 magmatic arcs, including the results from this study, show a trajectory of $\epsilon\text{Hf}/\text{Ma} =$
158 0.0232 and $^{176}\text{Lu}/^{177}\text{Hf} = -0.0014$ (Figure 3a). Values of the least trimmed squares robust
159 regression as calculated can be found in Supplementary Material A.

160 In comparison with other Proterozoic orogenies such as the collisional Grenville
161 ($\epsilon\text{Hf}/\text{Ma} = 0.0378$ and $^{176}\text{Lu}/^{177}\text{Hf} = -0.22$), and accretionary Sveconorwegian ($\epsilon\text{Hf}/\text{Ma} =$
162 0.0146 and $^{176}\text{Lu}/^{177}\text{Hf} = 0.012$) and Valhalla ($\epsilon\text{Hf}/\text{Ma} = \sim 0.0182$ and $^{176}\text{Lu}/^{177}\text{Hf}$
163 $= 0.007$), the Minas segment evolution arrays reflects a mixed collisional and accretionary
164 process in a collisional setting (e.g., Spencer et al., 2019).

165 **SIMILAR PHANEROZOIC HF MODEL RECORDED IN A** 166 **PALEOPROTEROZOIC OROGEN**

167 Two thousand four hundred and sixty-eight (n=2468) Hf analyses for the São
168 Francisco Craton, including the results from this work, were compiled in order to better
169 constrain the evolutionary trend of the Hf isotopic array of the Minas segment of the
170 Minas-Bahia Orogenic System.

171 Regarding the Archean complexes and associated passive margin Minas
172 Supergroup, in addition to the Piedade microcontinent, there are zircon grains in
173 magmatic rocks as old as ca. 3.2 Ga with positive to negative ϵHf values, and up to ca.

174 3.9 Ga detrital zircons with mainly negative ϵ_{Hf} values suggesting the presence of an
175 even older crust segment in this area. The Siderian to Rhyacian Mineiro and Juiz de Fora
176 and the Rhyacian Mantiqueira magmatic arcs display the isotopic trend array of a mixed
177 crustal-mantle signature, suggesting some degree of magmatic addition from the mantle
178 to the crust in the time span between ca. 2.4 Ga and 2.0 Ga with $\epsilon_{\text{Hf}}/\text{Ma}$ between 3.0 and
179 2.0 Ga of ~ 0.00255 (Figure 4a).

180 Accretionary episodes are characterized mostly by juvenile additions, whereas
181 collisional episodes of internal orogens lead to high reworking rates and large variation
182 in the negative ϵ_{Hf} values (Roberts and Spencer, 2015). Together, they are markers of
183 modern tectonic settings and depict how efficient mixing processes govern crustal
184 balance on Earth. Nonetheless, the variation with higher proportions of juvenile
185 signatures in the dataset present here, alongside a regional ϵ_{Hf} -time reworking array of
186 the regional Archaean rocks suggests that there was a change in between these periods
187 that is comparable to modern-tectonics, as shown by the $\epsilon_{\text{Hf}}/\text{Ma}$ trajectory of Archaean
188 and Paleoproterozoic rocks (Figure 4a).

189 The assembly of the Minas segment of the MBO resembles the Hf isotopic array
190 of the Phanerozoic internal orogenic systems of North China, South China and the
191 Himalayas with an $\epsilon_{\text{Hf}}/\text{Ma}$ trajectory of 0.00767 (collisional - Figure 4b) in contrast to
192 external orogenic systems of East Australia, Gondwana, Japan, New Zealand, South
193 America and Europe with $\epsilon_{\text{Hf}}/\text{Ma}$ trajectory of -0.0027 (accretionary – Figure 4c)
194 (Collins et al., 2011). Successive collisional orogenies of the Minas segment are
195 progressively younger towards the east (Figure 3), with subduction related magmatism
196 restricted to periods of ocean closure. The onset of accretionary and collisional episodes
197 throughout Earth history, from the Archaean-Proterozoic boundary, suggests the opening
198 and closure of oceans and provides important information regarding the formation of

199 supercontinent cycles (eg. Belousova et al., 2010; Collins et al., 2011; Hawkesworth et
200 al., 2016).

201 The increasing reworking rates and juvenile magmatic contributions at the
202 boundary between the Archaean and Paleoproterozoic marks a turning point in Earth
203 geodynamics. In the Archean, the lower contribution of juvenile magmatism, testified by
204 the less proportions of overall ϵHf values, forms a dominant crustal reworking array. In
205 the Paleoproterozoic, the proportion of juvenile magmas is enhanced in comparison to
206 the magmas derived from crustal reworking, which is analogous to the geodynamics of
207 modern plate tectonics.

208 **ACKNOWLEDGEMENTS**

209 The authors thank the facilities and the help from all the technical support of the
210 laboratories (LGPA, LAGIR) of the Geology Institute at UERJ, the Rio de Janeiro State
211 University, and the University of Portsmouth. We would like to thank Dr. William Clyde
212 for the editorial handling of the manuscript and three anonymous reviewers for their
213 contributions. We should thank FAPERJ and CNPq funding agencies.

214 **FIGURE CAPTIONS**

215 Figure 1: A) Tectonic Framework of Brazil (Modified after Heilbron et al., 2017); B)
216 Basement (Archean blocks and Paleoproterozoic magmatic arcs) of the São Francisco
217 Craton. (Modified from Alkmin and Teixeira, 2017; Barbosa and Barbosa, 2017; Degler
218 et al., 2018; Bruno et al., 2020); C) Geological map and location of studied samples
219 (Modified from Alkmin and Teixeira 2017; Bruno et al., 2021).

220 Figure 2: ϵHf vs. $^{207}\text{Pb}/^{206}\text{Pb}$ ages of analyzed magmatic zircon grain and metamorphic
221 rims; b) $^{176}\text{Hf}/^{177}\text{Hf}$ versus vs. $^{207}\text{Pb}/^{206}\text{Pb}$ ages of analyzed magmatic zircon grains and
222 metamorphic rims. Depleted Mantle area (DM) after Albert et al., (2016). All these

223 samples were previously dated via (LA-ICP-MS) U-Pb in zircon by Bruno et al. (2020)
224 and Bruno et al. (2021). CHUR constants of Bouvier et al. (2008) $^{176}\text{Hf}/^{177}\text{Hf} = 0.282785$
225 and $^{176}\text{Lu}/^{177}\text{Hf} = 0.0336$). Classifying fields of juvenile, moderately juvenile and evolved
226 from Bahlburg et. al., (2011).

227 Figure 3: Integrated tectonic evolution model for the Minas segment of the MBOS as
228 envisaged for the period between a) ca. 2.4 to 2.1 Ga and b) ca. 2.1 to 2.0 Ga (Modified
229 after Bruno et al., 2021) c) Zircon Hf data from the Paleoproterozoic rocks and trajectory
230 of $\epsilon\text{Hf}/\text{Ma}$ (Data from this study, Barbosa et al., 2015, 2019; Teixeira et al., 2015; Degler
231 et al., 2018; Moreira et al., 2018; Kuribara et al., 2019; Araújo, 2020). Depleted Mantle
232 area (DM) after Albert et al., (2016).

233 Figure 4: A) Hafnium isotopic signature of the Minas segment. (Data from this study,
234 Barbosa et al., 2015,2019; Teixeira et al., 2015; Albert et al., 2016; Moreira et al., 2016;
235 Martinez-Dopico et al., 2017; Degler et al., 2018; Moreira et al., 2018; Kuribara et al.,
236 2019; Cutts et al., 2020; Araújo, 2020). Samples from the Acaiaca, Pedra Dourada and
237 Minas Supergroup metasedimentary sequences are not considered for calculations of
238 trajectory of $\epsilon\text{Hf}/\text{Ma}$; B) Hafnium isotopic signature of Phanerozoic internal orogenic
239 systems (Collins et al., 2011 and references therein); C) Hafnium isotopic signature of
240 Phanerozoic external orogenic systems (Collins et al., 2011 and references therein.
241 Depleted Mantle area (DM) after Albert et al., (2016).

242 REFERENCES CITED

243 Albert, C., Farina, F., Lana, C., Stevens, G., Storey, C., Gerdes, A., Dopico, C. 2016.
244 Archean crustal evolution in the Southern São Francisco craton, Brazil:
245 Constraints from U-Pb, Lu-Hf and O isotope analyses. *Lithos* 266-267, 64-86.

246 Alkmim, F.F. and Teixeira, W., 2017. The Paleoproterozoic Mineiro belt and the
247 Quadrilátero Ferrífero. In: Heilbron M., Alkmim F., Cordani U.G. (Guest Ed.),
248 The São Francisco Craton and its margins, Eastern Brazil. Regional Geology
249 Review Series. Springer-Verlag, Chapter 5, 71–94.

250 Araújo, L.E.A.B. 2020. Tectonic evolution of the Juiz de Fora Complex: Siderian to
251 Rhyacian magmatic arc and its regional correlations within the Minas-Bahia
252 Orogen and the Western Central Africa Belt. [Ph.D. thesis]. Universidade do
253 Estado do Rio de Janeiro.

254 Ávila, C.A., Teixeira, W., Bongioiolo, E.M., Dussin, I.A., 2014. The Tiradentes suite and
255 its role in the Rhyacian evolution of the Mineiro belt, São Francisco Craton:
256 Geochemical and U-Pb geochronological evidence. *Precambrian Research*. 243,
257 221–251.

258 Barbosa, J.S.F. and Barbosa, R.G., 2017. The Paleoproterozoic Eastern Bahia Orogenic
259 Domain. In: Heilbron M., Alkmim F., Cordani U.G. (Guest Ed.), The São
260 Francisco Craton and its margins, Eastern Brazil. Regional Geology Review
261 Series. Springer-Verlag, Chapter 4, 57-70.

262 Barbosa, N.S., Teixeira W., Ávila C.A., Montecinos P.M., Bongioiolo E.M. 2015. 2.17–
263 2.10 Ga plutonic episodes in the Mineiro belt, São Francisco Craton, Brazil: U-
264 Pb ages, geochemical constraints and tectonics *Precambrian Research*. 270, 204-
265 225.

266 Barbosa, N.S., Teixeira, W., Ávila, C.A., Montecinos, P.M., Bongioiolo, E.M.,
267 Vasconcelos, F.F. 2019. U-Pb geochronology and coupled Hf-Nd-Sr isotopic-
268 chemical constraints of the Cassiterita Orthogneiss (2.47–2.41-Ga) in the Mineiro

269 belt, São Francisco craton: Geodynamic fingerprints beyond the Archean-
270 Paleoproterozoic Transition. *Precambrian Research* 326, 399-416.

271 Belousova, E.A. Kostitsyn Y.A., Griffin W.L., Begg G.C., O'Reilly S.Y., Pearson N.J.
272 2010. The growth of the continental crust: constraints from zircon Hf-isotope data.
273 *Lithos*, 119 (3–4), 457-466.

274 Bruno H., Elizeu V., Heilbron M., Valeriano C.M., Strachan R., Fowler M., Bersan S.,
275 Moreira H., Dussin I., Silva L.G.E.S., Tupinambá M., Almeida J., Neto C., Storey
276 C. 2020. Neoproterozoic and Rhyacian TTG-Sanukitoid suites in the southern São
277 Francisco Paleoproterozoic, Brazil: Evidence for diachronous change towards
278 modern tectonics. *Geoscience Frontiers* 11 (5), 11 (5), 1763-1787.

279 Bruno, H., Heilbron, M., Valeriano, C.M., Strachan, R., Fowler, M., Bersan, S., Moreira,
280 H., Motta, R., Almeida, J., Carvalho, M., Storey, C. 2021. The Rhyacian Minas-
281 Bahia Orogen, southern São Francisco Paleoproterozoic, Brazil: evidence for a
282 complex accretionary history preceding the amalgamation of Columbia.
283 *Gondwana Research* 92, 149-171.

284 Collins, W.J., Belousova, E.A., Kemp, A.I.S., Murphy, B. 2011. Two contrasting
285 Phanerozoic orogenic systems revealed by hafnium isotope data.
286 *Nature Geosciences* 4, 333-337.

287 Cutts, K., Lana, C., Moreira, H., Alkmim, F. Peres, G. 2020. Zircon U-Pb and Lu-Hf
288 record from high-grade complexes within the Mantiqueira Complex: First
289 evidence of juvenile crustal input at 2.4–2.2 Ga and implications for the
290 Palaeoproterozoic evolution of the São Francisco Craton. *Precambrian Research*
291 338, 105567.

292 Degler, R., Pedrosa-Soares, A., Novo, T., Tedeschi, M., Silva, L., Dussin, I., Lana. C.
293 2018. Rhyacian-Orosirian isotopic records from the basement of the Araçuá-
294 Ribeira orogenic system (SE Brazil): Links in the Congo-São Francisco
295 palaeocontinent. *Precambrian Research*. 317, 179-195.

296 Dhuime B., Hawkesworth C., Cawood P., Storey C. 2012. A change in the geodynamics
297 of continental growth 3 billion years ago. *Science*, 335, 1334-1336.

298 Goodge J.W., and Vervoort J.D. 2006. Origin of Mesoproterozoic A-type granites in
299 Laurentia: Hf isotope evidence. *Earth Planetary Science Letters* 243, 711-731.

300 Griffin, W.L., Pearson, N.J., Belousova, E., Jackson, S.E., van Achterberg, E., O'Reilly,
301 S., Shee, S.R. 2000. The Hf isotope composition of cratonic mantle: LAM-MC-
302 ICPMS analysis of zircon megacrysts in kimberlites. *Geochimica et*
303 *Cosmochimica Acta*. 64 (1), 133-147.

304 Hawkesworth, C.J., Cawood, P., Dhuime, B. 2016. Tectonics and crustal evolution. *GSA*
305 *Today*, 4-11.

306 Heilbron, M., Duarte B.P., Valeriano C.M., Simonetti A, Machado N, Nogueira, J.R.
307 .2010. Evolution of reworked Paleoproterozoic basement rocks within the Ribeira
308 belt (Neoproterozoic), SE-Brazil, based on U-Pb geochronology: Implications for
309 paleogeographic reconstructions of the São Francisco-Congo paleocontinent.
310 *Precambrian Research*. 178, 136–148.

311 Heilbron, M., Cordani, U.G., Alkmim, F.F. 2017. The São Francisco Craton and its
312 margins. In: Heilbron M., Alkmim F., Cordani U.G. (Guest Ed.), *The São*
313 *Francisco Craton and its margins, Eastern Brazil. Regional Geology Review*
314 *Series. Springer-Verlag, Chapter 1, 3-14.*

315 Kemp A.I.S., Hawkesworth C.J., Foster G.L., Paterson B.A., Woodhead J.D., Hergt J.M.,
316 Gray C.M., Whitehouse M.J. 2007. Magmatic and crustal differentiation history
317 of granitic rocks from hafnium and oxygen isotopes in zircon. *Science* 315, 980-
318 983.

319 Kuribara, Y., Tsunogae, T., Santosh, M., Takamura, Y., Costa, A.G., Rosière, C.A. 2019.
320 Eoarchean to Neoproterozoic crustal evolution of the Mantiqueira and the Juiz de
321 Fora Complexes, SE Brazil: Petrology, geochemistry, zircon U-Pb geochronology
322 and Lu-Hf isotopes. *Precambrian Research*. 323, 82-101.

323 Laurent, O. and Zeh, A. 2015. A linear Hf isotope-age array despite different granitoid
324 sources and complex Archean geodynamics: Example from the Pietersburg block
325 (South Africa). *Earth and Planetary Science Letter* 430, 326-338.

326 Martinez-Dopico C., Lana, C., Moreira, H.S., Cassino, L.F., Alkmim, F.F. 2017. U–Pb
327 ages and Hf-isotope data of detrital zircons from the late Neoproterozoic-
328 Paleoproterozoic Minas Basin, SE Brazil. *Precambrian Research* 291, 143-161.

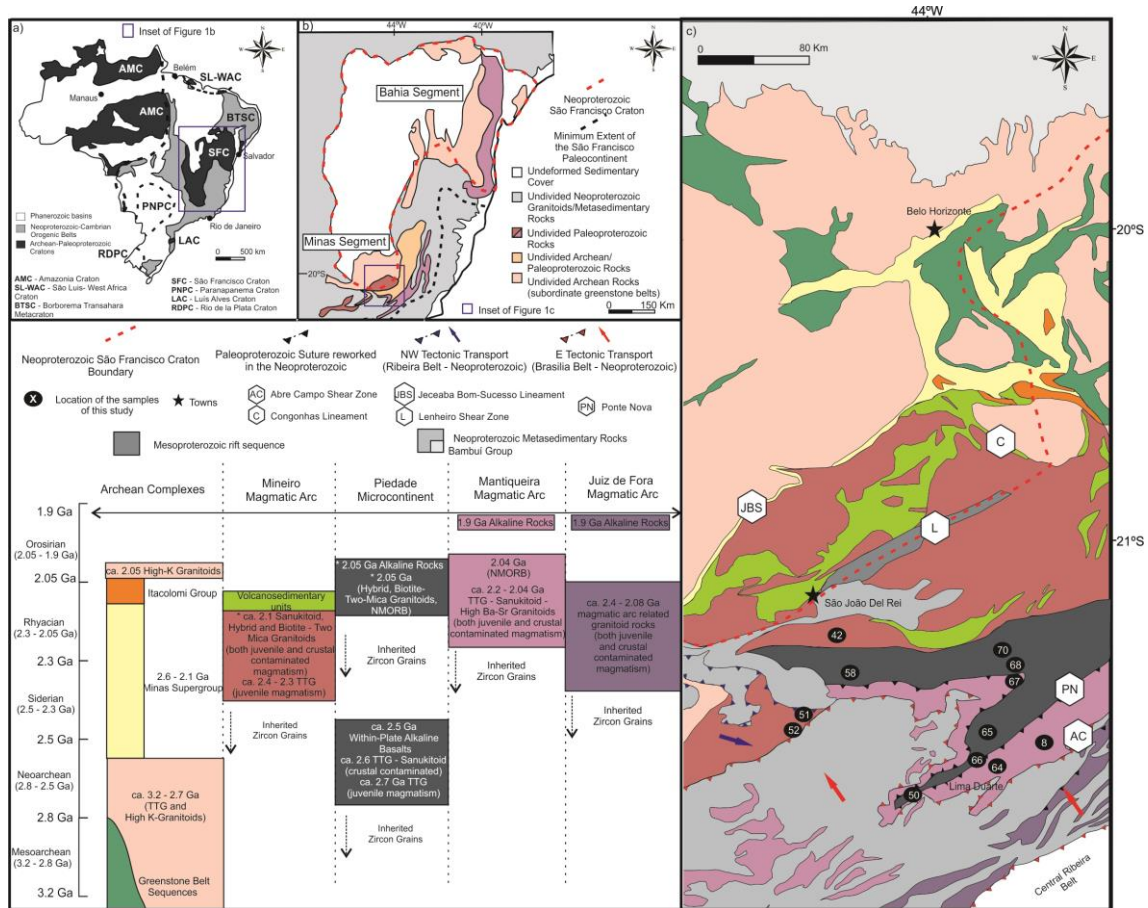
329 Moreira, H., Lana, C., Nalini Jr., H.A. 2016. The detrital zircon record of an Archaean
330 convergent basin in the Southern São Francisco Craton, Brazil. *Precambrian*
331 *Research* 275, 84-89.

332 Moreira H., Seixas L., Storey C., Fowler M., Lasalle S., Stevenson R., Lana C. 2018.
333 Evolution of Siderian juvenile crust to Rhyacian high Ba-Sr magmatism in the
334 Mineiro Belt, southern São Francisco Craton. *Geoscience Frontiers* 4, 977-995.

335 Palin, R.M., and Santosh, M. 2020. Plate tectonics: What, where, why, and when?
336 *Gondwana research*. <https://doi.org/10.1016/j.gr.2020.11.001>

- 337 Roberts, N. M. W., and Spencer, C. J. 2015. “The zircon archive of continent formation
338 through time” in *Continent Formation Through Time*. The Geological Society,
339 Vol. 389, eds N. M. W. Roberts, M. Van Kranendonk, S. Parman, S. Shirey, and
340 P. D. Clift (London: London Special Publication), p. 197–225.
- 341 Rudnick, R.L. and Gao S. 2003. Composition of the Continental crust. R.L. Rudnick
342 (Ed.), *The Crust Volume 3, Treatise on Geochemistry*, Pergamon, Oxford, 1-64.
- 343 Spencer, C.J., Kirkland, C.L., Prave, A.R., Strachan, R.A., Pease, V. 2019. Crustal
344 reworking and orogenic styles inferred from zircon Hf isotopes: Proterozoic
345 examples from the North Atlantic region. *Geoscience Frontiers* 10 (2), 414 -424.
- 346 Spencer, C.J., Kirkland, C.L., Roberts, N.M.W., Evans, N.J., Liebmann, J. 2020.
347 Strategies towards robust interpretations of in situ zircon Lu–Hf isotope analyses.
348 *Geoscience Frontiers* 11 (3), 843 – 853.
- 349 Teixeira, W., Ávila, C.A., Dussin, I.A., Neto, A.C., Bongioiolo, E.M., Santos, J.O.,
350 Barbosa, N.S., 2015. A juvenile accretion episode (2.35–2.32 Ga) in the Mineiro
351 belt and its role to the Minas accretionary orogeny: Zircon U–Pb–Hf and
352 geochemical evidence. *Precambrian Research*. 256, 148–169.
- 353 Teixeira, W., Oliveira, E.P., Marques, L.S. 2017. Nature and Evolution of the Archean
354 Crust of the São Francisco Craton. In: Heilbron M., Alkmim F., Cordani U.G.
355 (Guest Ed.), *The São Francisco Craton and its margins, Eastern Brazil*. Regional
356 *Geology Review Series*. Springer-Verlag, Chapter 3, 29-56.
- 357 Vervoort J.D. and Kemp A.I.S. 2016. Clarifying the zircon Hf isotope record of crust–
358 mantle evolution. *Chemical Geology* 425, 65-75.

361 **Figure 1**



362

363

364

365

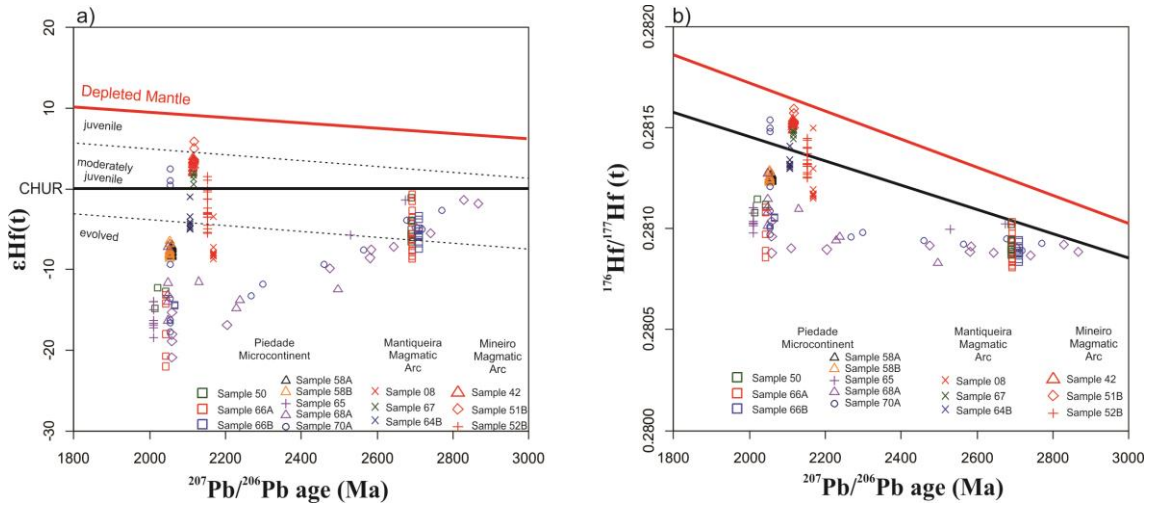
366

367

368

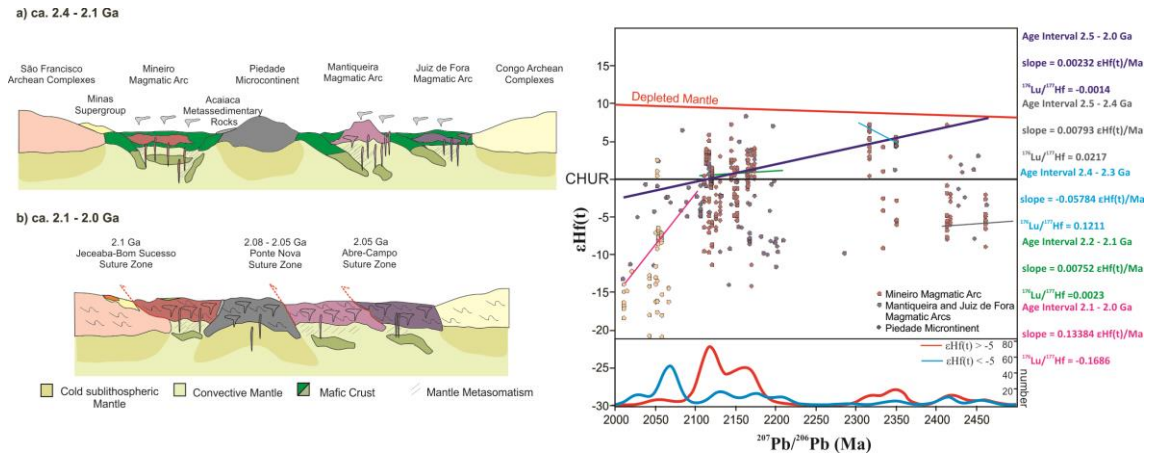
369

370 **Figure 2**



371

372 **Figure 3**



373

374

375

376

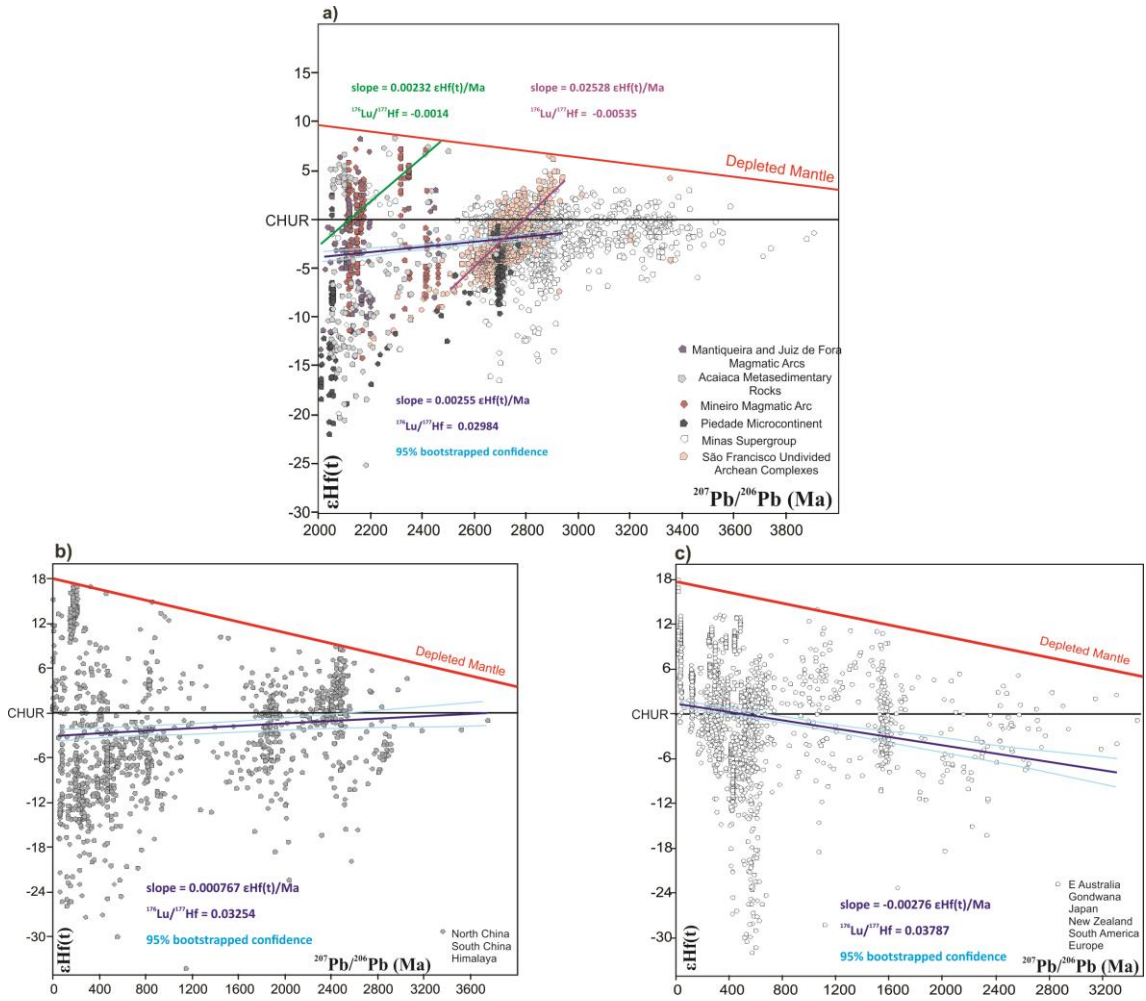
377

378

379

380

381 **Figure 4**



382

383